Experimental and Numerical Studies of Sound Propagation Over a Submarine Canyon Northeast of Taiwan

Ying-Tsong Lin, *Member, IEEE*, Timothy F. Duda, *Senior Member, IEEE*, Chris Emerson, Glen Gawarkiewicz, Arthur E. Newhall, *Member, IEEE*, Brian Calder, *Member, IEEE*, James F. Lynch, *Fellow, IEEE*, Philip Abbot, *Member, IEEE*, Yiing-Jang Yang, and Sen Jan

***Abstract*—A study of sound propagation over a submarine canyon northeast of Taiwan was made using mobile acoustic sources during a joint ocean acoustic and physical oceanographic experiment in 2009. The acoustic signal levels (equivalently, transmission losses) are reported here, and numerical models of 3-D sound propagation are employed to explain the underlying physics. The data show a significant decrease in sound intensity as the source crossed over the canyon, and the numerical model provides a physical insight into this effect. In addition, the model also suggests that reflection from the canyon seabed causes 3-D sound focusing when the direction of propagation is along the canyon axis, which remains to be validated in a future experiment. Environmental uncertainties of water sound speed, bottom geoacoustic properties, and bathymetry are addressed, and the implications for sound propagation prediction in a complex submarine canyon environment are also discussed.**

***Index Terms*—North Mien-Hua Canyon, submarine canyons, 3-D sound propagation.**

I. Introduction

An integrated physical oceanographic and ocean acoustic experiment, the Quantifying, Predicting and Exploiting (QPE) Uncertainty Initiative Experiment, was conducted northeast of Taiwan [1] in summer 2009. One of the research objectives was to study sound propagation over a submarine canyon and provide a better understanding of canyon bathymetric effects on acoustics. In addition, canyons are important due to the abundance of marine life and their role as conduits for water mass exchange between continental shelf and slope regions. The study site was located at the North Mien-Hua Canyon, whose topography is shown in Fig. 1. This canyon system cuts into the slope at the southern end of the Okinawa Trough, and there are four branches extending into the East China Sea Shelf.

Sound propagation in a submarine canyon can be profoundly influenced by the complexity of the canyon seafloor, and two QPE data collection efforts were dedicated to studying this subject in a real environment. The first effort resulted in the data set reported here, which was collected in the west branch of the North Mien-Hua Canyon on August 26 and September 8, 2009. The second effort was focused on an adjacent branch [2]. The west branch work presented in this paper is distinguished from the other work in a number of ways. First, it employed controlled acoustic sources to actively investigate the canyon acoustic effect, whereas in the adjacent branch, intensification of distant ship noise by the canyon seafloor was analyzed [2]. Second, the zigzag source tracks in the west branch study provided acoustic signal levels and transmission loss (TL) data with broader spatial coverage. Third, there are significant differences between the bathymetry in the two canyon branches, with the west branch being narrower and having steeper slopes.

Numerical simulation of 3-D sound propagation was performed before the QPE field work that clearly shows the effect of sound focusing caused by the canyon seafloor. This numerical simulation helped form the experimental design, and a brief summary of this work is provided in this paper. Also, the underwater environment in the North Mien-Hua Canyon area was characterized to provide an environmental model for acoustic studies. A bathymetric database with a 100-m spatial resolution was built by the Center for Coastal and Ocean Mapping/Joint Hydrographic Center at the University of New Hampshire (Durham, NH, USA). This bathymetric database was created from publicly available records made by single-beam and multibeam echo sounders in the region of interest. The source data contain a number of significant artifacts, which manifest themselves as irregular lines and tracks in a contour plot (see Fig. 1). To reduce these artifacts, a 2-D median filter [3] was implemented to construct a bathymetric map, where each grid

Manuscript received April 08, 2013; revised August 28, 2013; accepted November 20, 2013. Date of publication February 19, 2014; date of current version January 09, 2015. The Quantifying, Predicting and Exploiting (QPE) Uncertainty Initiative Experiment was supported jointly by the National Science Council, Taiwan, under Project NSC98-2623-E002-018-D and the U.S. Office of Naval Research (ONR) under Grant N00014-08-1-0763. The work of Y.-T. Lin was supported by the U.S. ONR under Grants N00014-10-1-0040 and N00014-13-1-0026. The work of T. F. Duda was supported by the U.S. ONR under Grant N00014-11-1-0194.

Associate Editor: G. Potty.

Y.-T. Lin, T. F. Duda, G. Gawarkiewicz, A. E. Newhall, and J. F. Lynch are with the Woods Hole Oceanographic Institution, Woods Hole, MA 02543 USA (e-mail: ytlin@whoi.edu; tduda@whoi.edu; ggawarkiewicz@whoi.edu; anewhall@whoi.edu; jlynch@whoi.edu).

C. Emerson and P. Abbot are with the Ocean Acoustical Services and Instrumentation Systems, Inc., Lexington, MA 02421 USA (e-mail: emerson@oasislex.com; abbot@oasislex.com).

B. Calder is with the Center for Coastal and Ocean Mapping, Chase Ocean Engineering Laboratory, Durham, NH 03824 USA (e-mail: brc@ccom.unh.edu).

Y.-J. Yang was with the Naval Academy, Kaohsiung City 813, Taiwan. He is currently with the National Taiwan University, Taipei 10617, Taiwan (e-mail: yjyang67@ntu.edu.tw).

S. Jan is with the National Taiwan University, Taipei 10617, Taiwan (e-mail: senjan@ntu.edu.tw).

Digital Object Identifier 10.1109/JOE.2013.2294291

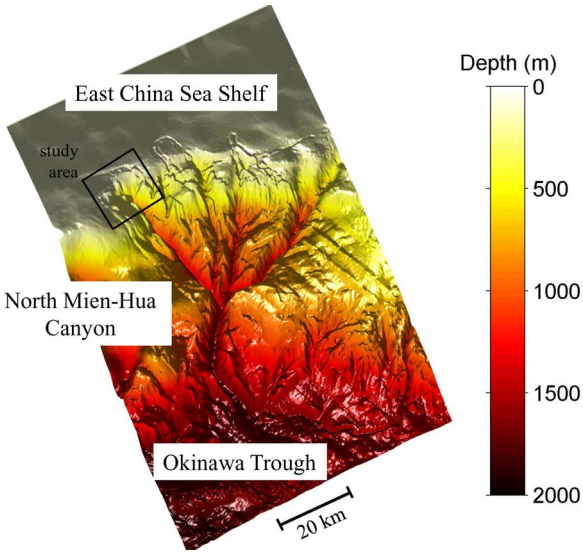

Fig. 1. Topography of the North Mien-Hua Canyon. The study area reported in this paper is marked by the box on the west branch. The bathymetric data are from a database (100-m resolution) built for the QPE experiment.

point contains the median value of the input bathymetric depths in the 250-m by 250-m neighborhood around the grid point. The canyon topography used in the acoustic models reported in this paper is shown in Fig. 2.

During the QPE experiment, onboard conductivity–temperature–depth (CTD) systems and a towed undulating SeaSoar vehicle equipped with CTD sensors were deployed to make volumetric measurements of water temperature and salinity, from which water sound speed was derived. The sound-speed measurements were then averaged spatially (15 km $\times$ 15 km) and temporally (daily) to create mean-state water sound-speed profiles in the study area of canyon acoustics on August 26 and September 8, 2009. The SeaSoar track and the locations of the CTD casts are shown in Fig. 2(a) and (b), and the mean sound-speed profiles are shown in Fig. 2(c). Detailed descriptions of the SeaSoar operations and the bathymetric database can be found in a QPE data report [4]. Finally, a model of homogeneous sandy bottom is assumed with sound speed 1700 m/s, density 1.5 g/cm^3, and attenuation coefficient 0.5 dB/λ. The assumption underlying this bottom model is based on the strong near-bottom currents in the North Mien-Hua Canyon, which make fine suspended sediments unlikely to settle, resulting in a sandy bottom. A brief discussion will be provided concerning bottom property uncertainty in the environmental model for our acoustic studies.

This paper is organized as follows. The numerical and experimental methods are reviewed in Section II. The numerical simulations before the field work and the experimental results are presented in Section III along with 3-D sound propagation models. Discussions of the experimental and environmental uncertainties and the effects on sound propagation prediction/modeling are provided in Section IV. The paper concludes in Section V along with suggestions for future work.

II. Methods

The numerical program employed for modeling sound propagation and the performance of the acoustic equipment used in this study are reviewed in this section.

A 3-D parabolic equation (PE) model using the split-step Fourier (SSF) algorithm [5] with a wide-angle PE approximation [6] was utilized in this study. This 3-D PE model can be implemented in either a Cartesian or a cylindrical coordinate system [7], [8], and the solution of sound pressure is obtained with a one-way marching algorithm originating from the source position. The advantage of using a Cartesian coordinate in the numerical scheme is that the model resolution is uniform over the computational domain, but its PE approximation errors will increase with azimuth angle. Lin *et al.* [8] have found that the Cartesian 3-D PE can provide a valid approximation within $\pm 20^\circ$ in azimuth, and so it is good for modeling long-range, plane-wave-like sound propagation. On the other hand, the cylindrical PE model holds a consistent degree of approximation along radials from the source at each azimuth, but the conventional fixed cylindrical grids will not have uniform model resolution. Two methods have been proposed by Lin *et al.* [8] to improve cylindrical PE model resolution: 1) utilizing an arc-length grid; and 2) extending angular wave number spectra with zeros (zero-padding). In the arc-length gridding method, the grid interval is fixed so the model resolution can be maintained in the far field. Because the arc-length aperture is also fixed, the model grid will wrap around the entire 360° azimuth near the source and gradually unwrap as the radius increases, which enables the model to capture all possible signals arriving at the area of interest. Since the arc-length gridding does not allow a fast Fourier transform [8], it will benefit the total model efficiency to switch the arc-length grid to the angular grid when the PE marching algorithm reaches a certain distance. This changeover of grids is seamless because both grids have cylindrical geometry. When the computation switches to the angular grid, the zero-padding technique is used to maintain the model resolution by extending the angular wave number spectra with zeros. The calculation cost is higher in the cylindrical 3-D PE model, partly because the free propagation operator needs to be updated at each marching step, unlike the Cartesian situation. Nevertheless, the cylindrical model provides a wider azimuthal aperture, and so it is good for modeling TL data with broad spatial coverage, as in the current study.

The acoustic signals were transmitted from a small, expendable unmanned underwater vehicle equipped with a broadband acoustic source, developed by Ocean Acoustical Services and Instrumentation Systems (OASIS), Inc. (Lexington, MA, USA) called the OASIS Mobile Acoustic Source (OMAS) [9]. The OMAS vehicle is 12.4 cm in diameter, 91.4 cm long, and weighs 10 kg. It can follow preset run geometries by varying course, depth, and speed while transmitting various acoustic waveforms. The OMAS vehicle can also be tracked in real time by means of time synchronizing the source with hydrophone receivers, thereby enabling the calculation of source range from the measured time delay between signal transmission and reception. The bearing information is obtained with use of a direction finding acoustic receiver (DIFAR) sonobuoy. More detailed description of the OMAS vehicle can be found in [9].

The OMAS vehicles used in the canyon study had a calibrated source level (SL) of $\sim$150 dB re 1 μPa at 1 m from 800 to 1000 Hz. The calibration showed that the vehicle's SL had a small

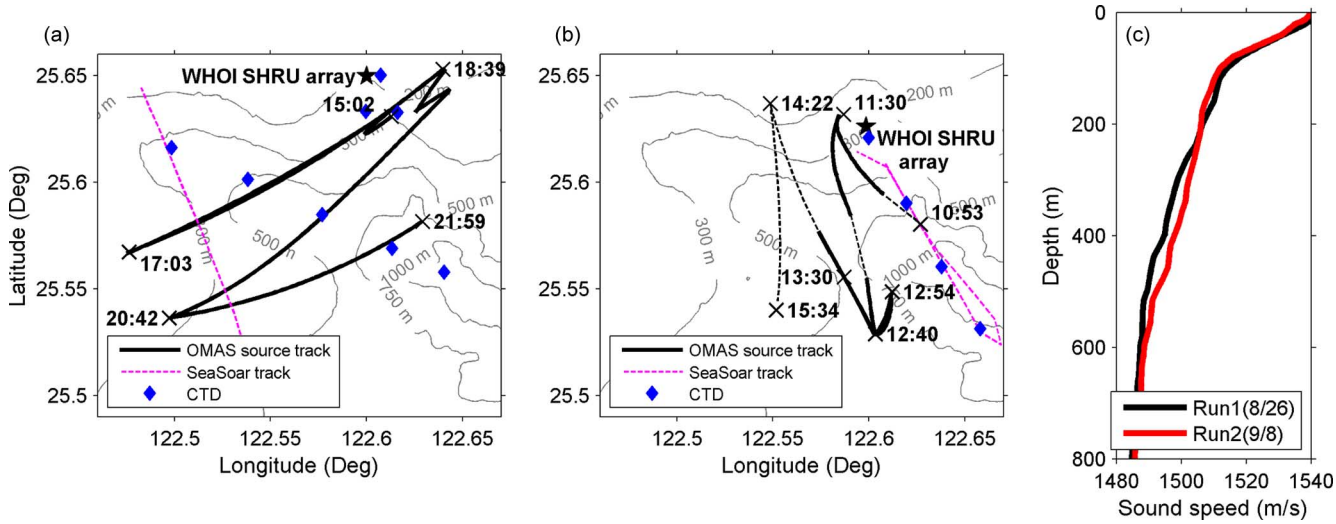

Fig. 2. (a) and (b) Outlines of the canyon acoustics experiments conducted on August 26 and September 8. (c) Average sound-speed profiles derived from the SeaSoar data and the shipboard CTD casts in the study area. The source tracking in Run 2 was interrupted (denoted with dashed lines) by ship noise.

ping-to-ping variability (<0.25 dB), and its sensitivity to the vehicle battery load was less than 0.5 dB over a 4-h test cycle.

The acoustic data shown in this paper were recorded by the several hydrophone receiver units (SHRU) system developed at the Woods Hole Oceanographic Institution (WHOI, Woods Hole, MA, USA). The SHRU was equipped with four hydrophones with a sensitivity equal to 170 dB μPa/V. The hydrophones were attached to the mooring cable away from the electronics package at different depths to create a vertical line array (VLA). The mooring was 20 m long, and was mounted on the seafloor. The sampling rate of this array system was 9765.625 Hz, and continuous records were made during the operation. Additional information can be found in the QPE data report [4].

III. Results

Numerical simulations with the 3-D PE model were carried out before the experiment to provide some guidelines for the field work. This numerical study and the canyon TL experiment data are presented in this section. The received levels of OMAS continuous-wave (CW) tones on SHRU hydrophones will also be shown, along with the acoustic models built for explaining sound propagation physics in the experimental area.

A. Numerical Simulation Before the Field Work

A number of numerical simulations for 3-D sound propagation in the North Mien-Hua Canyon were carried out. A strong focusing effect was found along the canyon axis. One example of the simulations is shown in Fig. 3, where the modeled source was placed at 25° 35.4′ N and 122° 37.2′ E (water depth ∼580 m), and a downward-refracting sound-speed profile similar to the ones shown in Fig. 2(c) was used. The explanation and implication of this modeling work are provided below.

Because we are interested in the sound field along the canyon axis within a small azimuth aperture in this pre-experimental study, the Cartesian 3-D PE model is appropriate. A 0-dB point source transmitting 600-Hz CW sound was considered, so the nominal acoustic wave length λ_0 was 2.5 m. The source depth was at 61 m. A bathymetric model was constructed using the

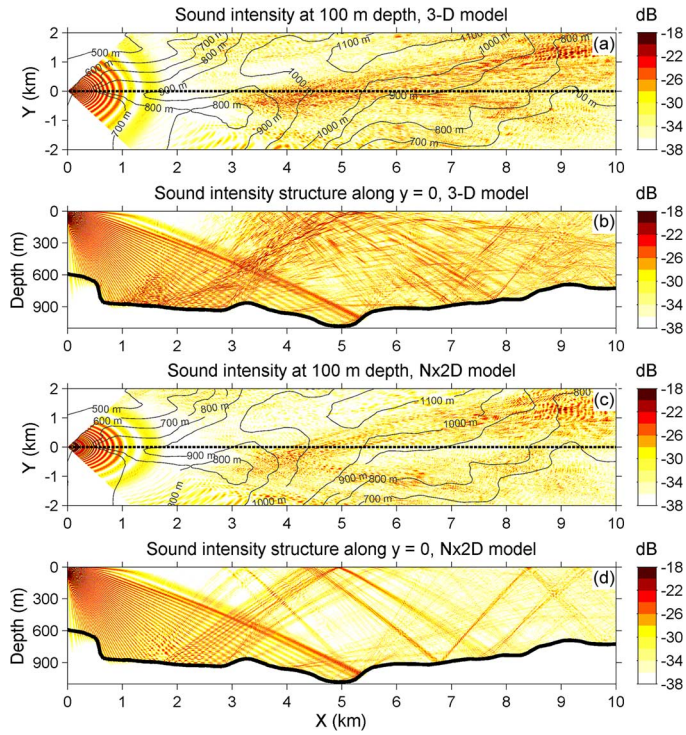

Fig. 3. Three-dimensional and $N\times$ 2-D numerical models of sound propagation in the North Mien-Hua Canyon. A 0-dB point source transmitting 600-Hz CW sound is considered. The source depth is 61 m. Cylindrical spreading loss is factored out to reduce the dynamic range of sound intensity in the plot.

QPE bathymetric database described in Section II, and it is shown in Fig. 3 as isobath contours. To capture the complexity of the canyon seafloor, the bathymetry was updated every 2.5 m (1.0 λ_0) in x (the PE marching direction) using interpolation. The grid sizes in y (transverse direction) and z (vertical depth) were set to be 0.625 m (one fourth of λ_0) and 0.417 m (one sixth of λ_0), respectively. The computation domain was a 10-km × 5.3-km × 4.1-km $(x - y - z)$ volume. The 4.1-km extent in z was chosen for employing an image field to satisfy the pressure-release boundary condition at the sea surface. In addition, an artificial absorbing layer was implemented around the $y - z$ mesh, and the final effective model domain below the

sea surface in y and z is about 4 km $\times$ 1.5 km. The convergence of the PE solution was ensured with a test using a PE marching step in x of 1.25 m.

In addition to the 3-D modeling, 2-D simulation with the same PE technique but neglecting the transverse variation of the seafloor and only considering its variation in the radial direction (termed $N\times$ 2-D in the literature) was carried out to identify the 3-D sound propagation effects caused by the canyon topography. Both 3-D and $N\times$ 2-D simulation results are shown in Fig. 3. Note that the 3-D simulation predicted stronger bottom reflection from the concave seafloor located at x =1–3 km and $y = 0$. This strong reflection is indeed caused by the out-of-plane reflection, which can only be captured by the 3-D model because it accounts for horizontal coupling in the y-direction, and the intensification of sound due to the focusing effect observed in the model is as much as 15 dB.

B. Canyon Acoustics Experiments

The acoustic field work utilizing the OMAS sources in the QPE 2009 experiment was performed on two days, August 26 and September 8. The acoustic data shown in this paper were recorded by WHOI SHRU VLAs. The hydrophone arrays were mounted at different locations in these two canyon acoustics experiments, but both were on the bottom with hydrophones located at 18, 13.6, 9.3, and 5.0 m above the seafloor, capturing acoustic signals at the very bottom of the water column. The first mooring location was at 25° 38.993′ N and 122° 36.014′ E ($\sim$225 m deep), and the second location was at 25° 37.563′ N and 122° 35.924′ E ($\sim$337 m deep).

During the first canyon experiment on August 26, two OMAS source vehicles were deployed, but only one, designated Run 1 in this paper [Fig. 2(a)], had useful signal reception on SHRU hydrophones. During the second canyon experiment on September 8 [Fig. 2(b)], one OMAS source vehicle was deployed (Run 2), and the signal reception on SHRU hydrophones was fair. In both experiments, the OMAS vehicles were moving at a speed of 5 kn at designated depths. The vehicle depth in Run 1 was at 50 m initially and changed to 100 m after 210 min to measure TL from a different source depth. In Run 2, the vehicle depth was set to a constant depth of 100 m. The sound source on the vehicle transmitted three 2-s hyperbolic frequency-modulated (HFM) sweeps from 800 to 1000 Hz, followed by another three 2-s HFM sweeps from 550 to 650 Hz. After transmitting the HFM chirps, the OMAS emitted 48-s CW tones at 780, 880, and 980 Hz in Run 1 and 800, 900, and 1000 Hz in Run 2 with a consistent source level of about 140.5 dB at each transmitted frequency. The entire transmission was 1 min in duration and repeated continuously.

One purpose of the HFM chirps was for source tracking from the sonobuoys to determine range and bearing. Note that, in Run 2, because of loud ship noise, the sonobuoy reception in the first hour was not strong enough to determine the signal direction, and a triangulation was implemented to locate the OMAS source using chirp arrival times at the sonobuoys and one SHRU hydrophone.

One of the experimental plans was to have the mobile source pass through a focal point in the canyon as predicted by the numerical simulation. This was implemented in Run 2, and the planned source track was along the SeaSoar and CTD track shown in Fig. 2(b). However, due to strong currents in the canyon, the actual source track was shifted away from the planned track. In Run 1, the source vehicle was programmed to go across the canyon along a linear track repeatedly for six hours. The OMAS course was maintained for three and a half hours before the current in the experimental area changed the direction and pushed the vehicle southeastwards. Although the OMAS tracks in both Run 1 and Run 2 did not follow the plans, the zigzag paths did result in a broader spatial coverage over the canyon.

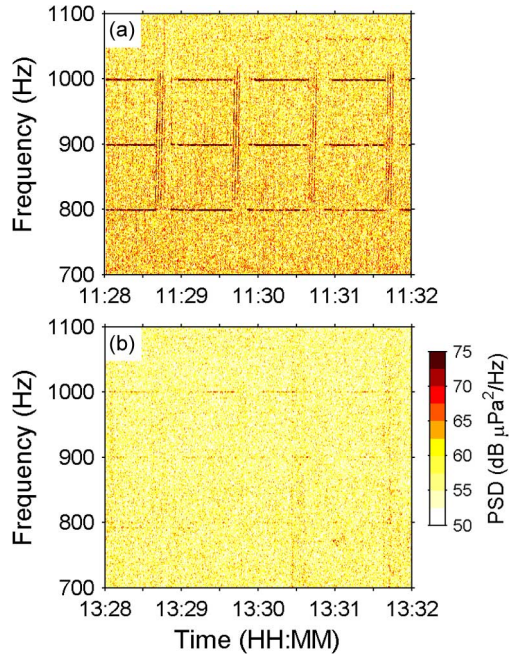

Fig. 4. Spectrograms of the received signals on the top hydrophone of the WHOI SHRU array at two different times: (a) 11:30:00 UTC; and (b) 13:30:00 UTC on September 8, 2009.

Two example spectrograms of the OMAS signals recorded on a SHRU hydrophone are presented in Fig. 4. The upper panel shows the records with high signal-to-noise ratio (SNR) at around 11:30:00 Coordinated Universal Time (UTC) in Run 2 when the source was close to the SHRU array. The lower panel of Fig. 4 shows the records with low SNR at around 13:30:00 UTC during the same run. Note that the ambient noise field varied significantly in time during this TL field experiment, and the noise level at 13:30:00 UTC was lower than at 11:30:00 UTC. Further discussion on the ambient noise will be provided later in this section.

The short-time Fourier transform (STFT) was employed to search for the OMAS CW signals in the SHRU data. In each STFT step, a 2-s-long signal (equivalently $\sim$5 m in distance as the OMAS vehicle was moving at a speed of 5 kn) was extracted and tapered using a Hamming window. It was then zero padded to 2^{17} points ($\sim$13.4 s long) for the Fourier transform to produce a high-resolution spectrum. Spectral peaks were sought within $\pm$4 Hz around the nominal signal frequencies (780, 880, and 980 Hz in Run 1, and 800, 900, and 1000 Hz in Run 2). Both the peak locations and the heights were recorded to determine the signal frequencies and the sound pressure levels (SPLs), which were taken to be the average of the true values within the 2-s

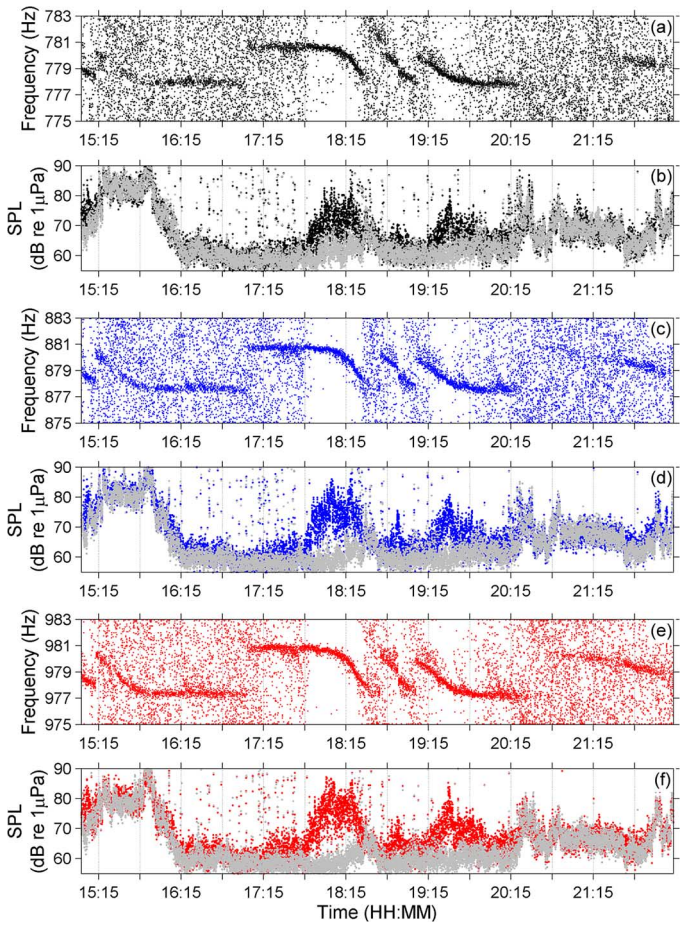

Fig. 5. Results of STFT signal processing for the OMAS CW tones recorded on the second hydrophone of the SHRU array in the canyon acoustics experiment on August 26 (Run 1). The top two panels are for the 780-Hz CW tone: (a) the peak frequencies searched from 775 to 783 Hz; and (b) the sound pressure levels at the peak frequencies. Other panels are for (c) and (d) the 880-Hz CW tones and (e) and (f) the 980-Hz CW tones. The gray dots are noise levels estimated in the frequency bands 10 Hz below the signal frequency ranges.

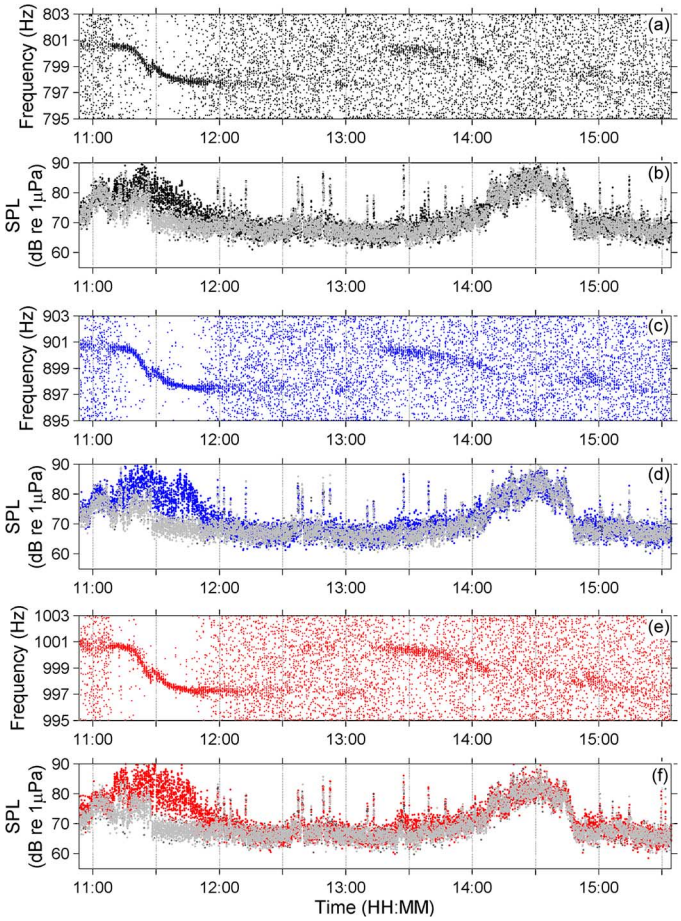

Fig. 6. Results of STFT signal processing for the OMAS CW tones recorded on the second hydrophone of the SHRU array in the canyon acoustics experiment on September 8 (Run 2). The top two panels are for the 800-Hz CW tone: (a) the peak frequencies searched from 795 to 803 Hz; and (b) the sound pressure levels at the peak frequencies. Other panels are for (c) and (d) the 900-Hz CW tones and (e) and (f) the 1000-Hz CW tones. The gray dots are noise levels estimated in the frequency bands 10 Hz above the signal frequency ranges.

(5-m) window. The 2-s STFT window was moved through the entire data set with a 1-s interval to obtain time series of signal frequencies and levels. The results from both runs are shown in Figs. 5 and 6. When the SNR was high, the STFT process would track the CW signals well, as seen in the Run 1 data (Fig. 5) from 17:45:00 to 18:30:00 UTC and in the Run 2 data (Fig. 6) from 11:15:00 to 11:50:00 UTC. However, when the SNR was low, the signals could not be tracked, and the peak frequencies would scatter over the search area. The concentration of the peak frequencies certainly depends on the SNR, and when there was small signal excess (an intermediate SNR), the peak frequencies would be somewhat condensed as seen, for example, at around 13:30:00 in Run 2 (Fig. 6).

To assess the ambient noise level, the same STFT process was performed but for frequency bands that are 10 Hz away from the signal frequency search ranges. The noise levels are plotted in Figs. 5 and 6 as gray dots, and the relation between the SNR and the signal tracking can be clearly seen. One can also see occasional high ship noise of up to 90 dB and a higher ambient noise condition in Run 2. It should be noted that the noise level estimates shown here are not the average levels over the bandwidth, but are peak levels. Distributions of the noise levels are shown in Fig. 7 for both runs, and the median noise level on August 26 (Run 1) was ∼7 dB lower. Since the major component of ambient noise in this frequency band is wind wave noise [10], the surface wind on August 26 should be slower. A record of averaged surface wind speeds in the experimental area, shown in Fig. 8, indeed confirms that.

C. *Acoustic Models*

The 3-D cylindrical SSF PE model was utilized to model the propagation of OMAS CW tones. Large azimuth angles were covered with consistent model accuracy at each azimuth. The principle of reciprocity was invoked, so the locations of the source and receiver were switched in the model, and the PE starter, mimicking a 0-dB point source, was placed at the WHOI SHRU location. Doppler shift due to the relatively slow vehicle movement (5 kn, ∼600 times slower than the sound speed in water) was neglected in the PE model, and the model frequencies were fixed at the nominal frequencies. A combined algorithm utilizing the methods of arc-length gridding and zero-padding angular wave-number spectrum [8] was employed to ensure that the model grid size in azimuth was always smaller than one half of the nominal wavelength λ_0. The details of this

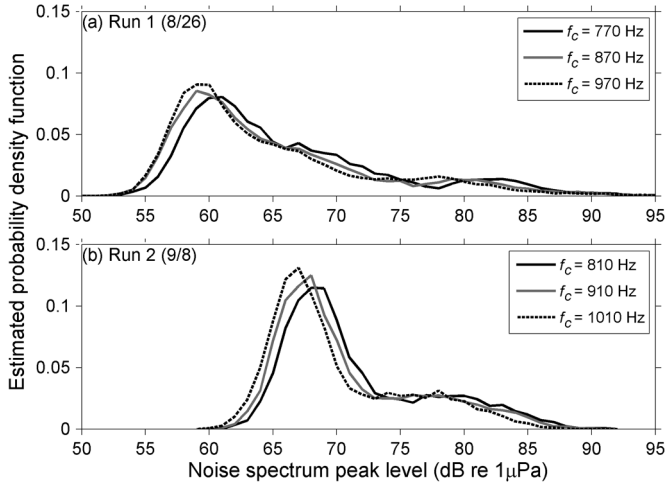

Fig. 7. Distributions of the noise spectrum peak levels received on the SHRU array over an 8-Hz band centered at the listed frequency during two canyon acoustics experiments in the North Mien-Hua Canyon.

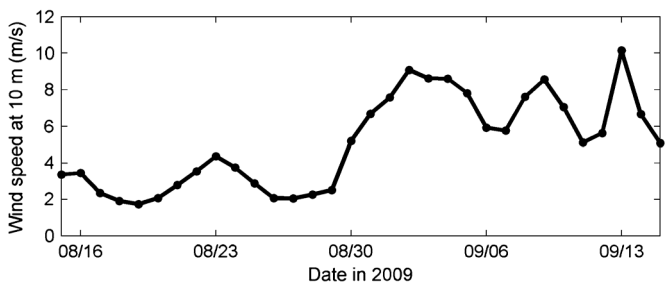

Fig. 8. Record of averaged surface wind speeds in the area of the QPE canyon acoustics experiments. The wind record was obtained from the Blended Sea Winds project [11], [12] in the National Climatic Data Center of the National Oceanic and Atmospheric Administration (http://www.ncdc.noaa.gov/oa/rsad/air-sea/seawinds.html).

combined algorithm are described in Section II. The model grid size in depth was set to be less than one third of λ_0, and the marching step was one half of λ_0. Artificial absorbing layers were implemented on the sides of computation domains to imitate the radiation boundary condition, and the bathymetry in the PE model was updated every four marching steps to capture the complexity of the canyon seafloor. The environmental information reviewed in the Introduction was used in the model, including the average water sound-speed profiles, the bathymetric model synthesized from historic data, and the homogenous sandy bottom model.

During the two transmission runs, OMAS vehicles were deployed to follow linear tracks across and along the canyon axis, but the vehicles were pushed away from the planned tracks by strong currents in the canyon. As a result, they traveled over the head of the canyon with zigzag paths (see Fig. 2) covering a much broader area. As shown in Figs. 5 and 6, detection of OMAS signals by the STFT process performed very well during high SNR periods. The detected frequencies indeed followed the OMAS vehicle's movement. To show that, theoretical frequencies with the Doppler shift were calculated using the OMAS tracking results, and they are shown in Fig. 9 to compare with the detected frequencies. A good agreement is observed, even during intermediate SNR periods. This good comparison of the Doppler shift also implies the OMAS vehicle tracking results are reliable.

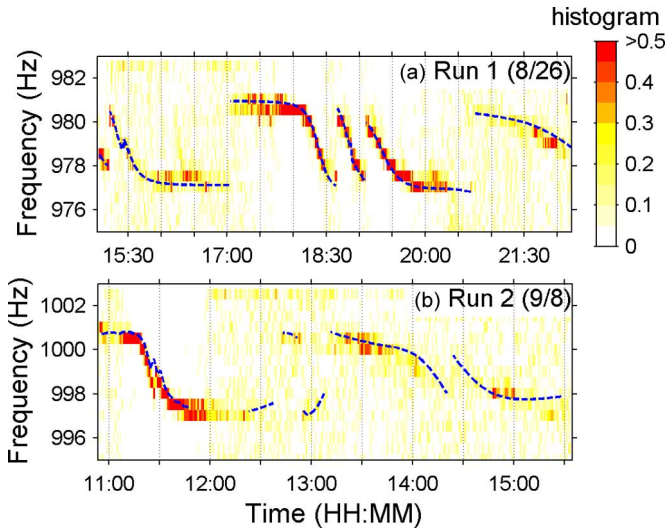

Fig. 9. Shaded image shows the histograms of the peak frequencies detected in the SHRU data for the OMAS CW signals at each minute. The dashed lines are the theoretical frequencies with the Doppler shift calculated using the OMAS tracking results.

The modeled TL on the horizontal planes at the OMAS vehicle depths during the high SNR periods in both OMAS transmission runs is shown in Figs. 10(a) and 11(a), respectively. The modeled TL along the vehicle tracks will also be compared with the measured TL data to assess the model performance. There are indeed model uncertainties, and they are in the specification of: 1) seafloor bathymetry; 2) water–column sound speed; and 3) bottom geoacoustic properties. Also, the OMAS vehicle tracking might potentially produce position errors. Detailed investigation of these model uncertainties is deferred to the future, but brief discussions will be provided in this paper. The 3-D sound propagation model presented here is meant to provide a first-order understanding of the sound propagation in the North Mien-Hua Canyon, which can also be generalized to other canyon systems.

The OMAS Run 1 transmission started at 15:02:00 UTC on August 26 (the times indicated hereafter are UTC), and the source track is shown in Fig. 2(a) with time stamps. Loud ship noise appeared in the acoustic records until 16:15:00. During this noisy period, the OMAS was close to the SHRU array, so there was still some signal excess for the STFT processor to detect the signals, as shown in Fig. 5. Good SNR data were obtained from 17:45:00 to 18:10:00, which will be used to assess the performance of the 3-D PE model. During this high SNR period, the OMAS was in fact leaving an acoustic shadow zone over the sloping bottom. The formation of the shadow zone was caused mainly by the downward-refracting sound-speed profiles in the area [see Fig. 2(c)], and the propagation condition over the sloping bottom was only favorable for deep sources, which will be discussed in detail later in this section.

Fig. 10 shows a 980-Hz TL comparison between the data and the model. There were 48-s CW signals emitted from the OMAS sources every minute, and a 30-s-long subsection was taken for signal processing, yielding 30 measurements of signal frequencies and SPL. So, each group of points in Fig. 10(b) spans 30 s, over which the OMAS vehicle moved ∼75 m in distance. The variability (standard deviation) of the logarithmic TL values is

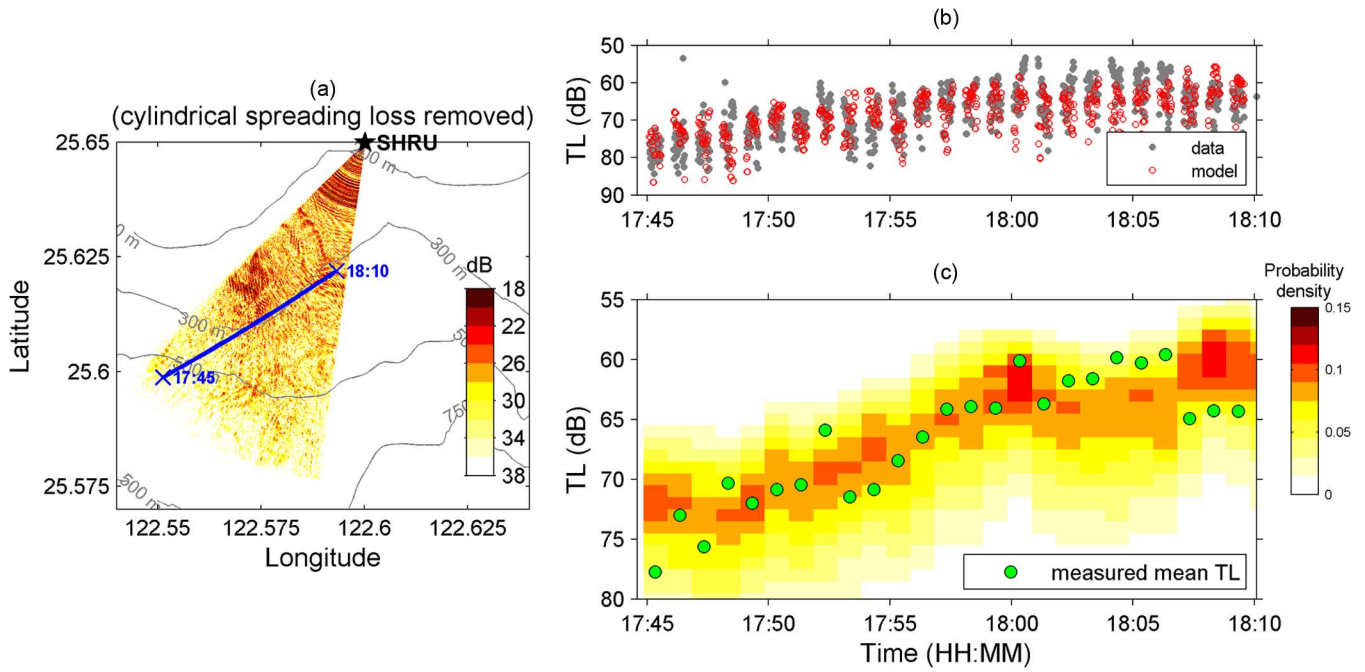

Fig. 10. Three-dimensional PE model TL and data comparison for the OMAS Run 1 980-Hz CW transmission (source depth 50 m): (a) a model TL contour; (b) a comparison scatter plot; and (c) a comparison of measured mean TL and modeled TL pdfs. The model pdfs are calculated from uncertain OMAS vehicle positions in a 1-min interval. Only the data with high SNR are considered.

∼3.5 dB on average, which is less than the expected 5.6 dB for a fully saturated CW phase-random situation [13]. This reduction is due to the moving average procedure in the STFT process, which in our current application utilizes a 2-s (equally 5 m in distance) moving window as explained in Section III-B. To compare the model variability with the data correspondingly, the model output needs to be averaged, and this is done at each PE marching step along the arc in our calculation.

As shown in Fig. 10(b), the modeled TL agrees with the measured data quite well in terms of the general trend and the variability. However, given the level of detail and accuracy in the environmental models and the OMAS track, it is not possible to perform a point-to-point comparison. So, in addition to the scatter plot of Fig. 10(b), we also present a comparison between the modeled TL probability density functions (pdfs) and the measured TL data in Fig. 10(c). The modeled TL pdfs were calculated and plotted every minute to show the distribution of the modeled TL ensemble at all possible OMAS positions within a 30-s window. The assumption is that the true OMAS positions in the 30-s window were within a radius of 150 m from the estimated location at the middle of the time window. Because the root mean square (RMS) errors of the OMAS track are on the order of 150 m, this assumption is reasonable. In addition, the OMAS vehicle traveled ∼75 m in 30 s, so the area of possible OMAS positions given by a radius of 150 m should also cover the vehicle path. We also consider uncertain vehicle depths with an error range of ±1 m when calculating the pdfs.

To show the agreement of the modeled TL trend, the measured mean TL data are superimposed on top of the modeled TL pdfs in Fig. 10(c). Each measured mean data point was calculated from the average amplitude of the CW signals in the same 30-s time window for computing the model pdf. A good agreement is observed, and the peaks of modeled pdfs follow the measured mean data points. The measured and modeled TL at 1000 Hz were compared in a similar way during the second OMAS run, and the plots shown in Fig. 11 present a good agreement between the two.

The Run 2 transmission started at 10:53:00 on September 8, and the SNR on the SHRU array was very low initially (see Fig. 6). This was partially due to the occurrence of loud ship noise, and also because the OMAS vehicle was in the SHRU's shadow zone. The OMAS signals started to be detected at 11:10:00 (see Fig. 6). The sound propagation model shown in Fig. 11(a) suggests that the OMAS vehicle left the shadow zone over the sloping bottom at this time, and the TL decreased to ∼57 dB, which is confirmed in the measured data. The model also shows that the OMAS reentered the shadow zone at ∼11:40:00, and, as shown in Fig. 11(b) and (c), which is confirmed in the measured data as well.

The PE model domain was extended to simulate sound propagation over a broader area. The OMAS Run 2 configuration was considered, and the model frequency was 800 Hz. Fig. 12(a) shows the modeled TL to the SHRU location within a radius of 11 km. The SPL cutoff range (∼3 km) due to the shadowing effect is similar to the 1000-Hz case seen in Fig. 11(a). The interference patterns at these two frequencies are, in fact, also similar. The TL across the center of the domain [Fig. 12(b)] clearly shows the shadow zone structure. The formation of the shadow zone was caused mainly by the downward-refracting sound-speed profiles in the area [see Fig. 2(c)], and Fig. 12(b) shows that the propagation condition is only favorable for deep sources. When the sound propagates across the canyon, the propagation scenario becomes up-slope, and this causes sound to bounce back to the upper water column and terminate the shadow zone, as observed in Fig. 12(a) and (b). The strength of this bottom interacting sound depends strongly on the slope

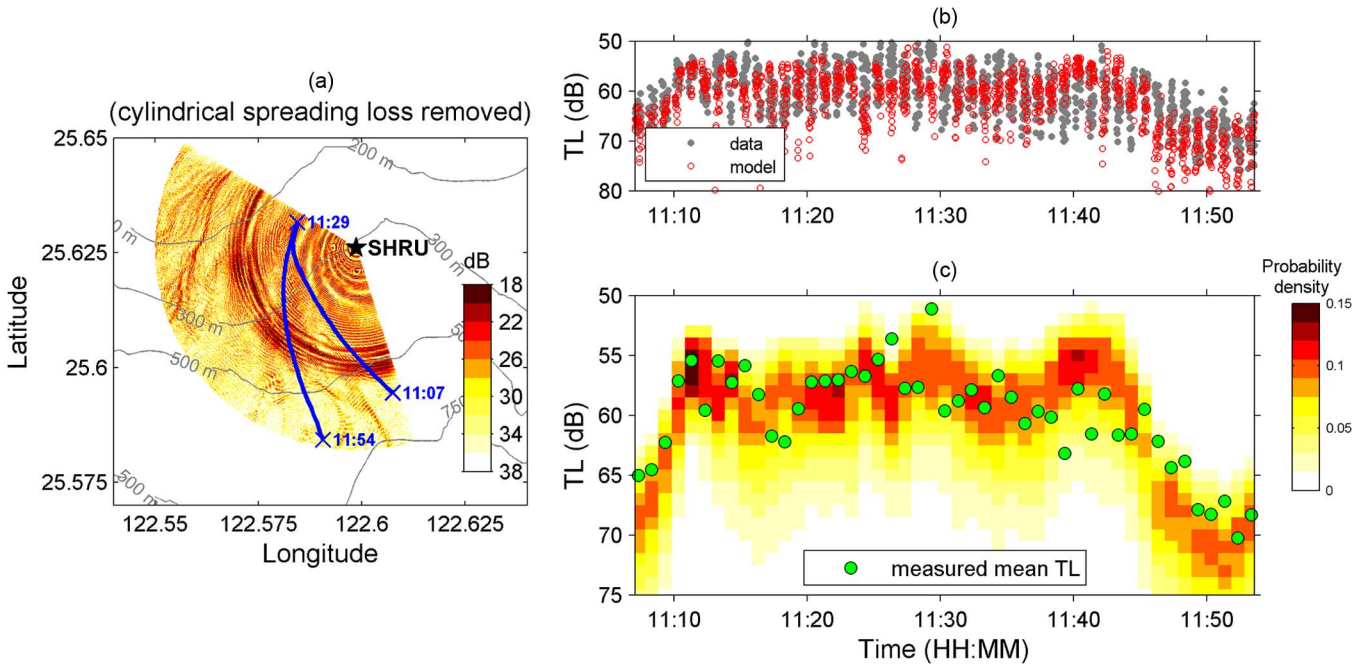

Fig. 11. Three-dimensional PE model TL and data comparison for the OMAS Run 2 1000-Hz CW transmission (source depth 100 m): (a) a model TL contour; (b) a comparison scatter plot; and (c) a comparison of measured mean TL and modeled TL pdfs. The model pdfs are calculated from uncertain OMAS vehicle positions in a 1-min interval. Only the data with high SNR are considered.

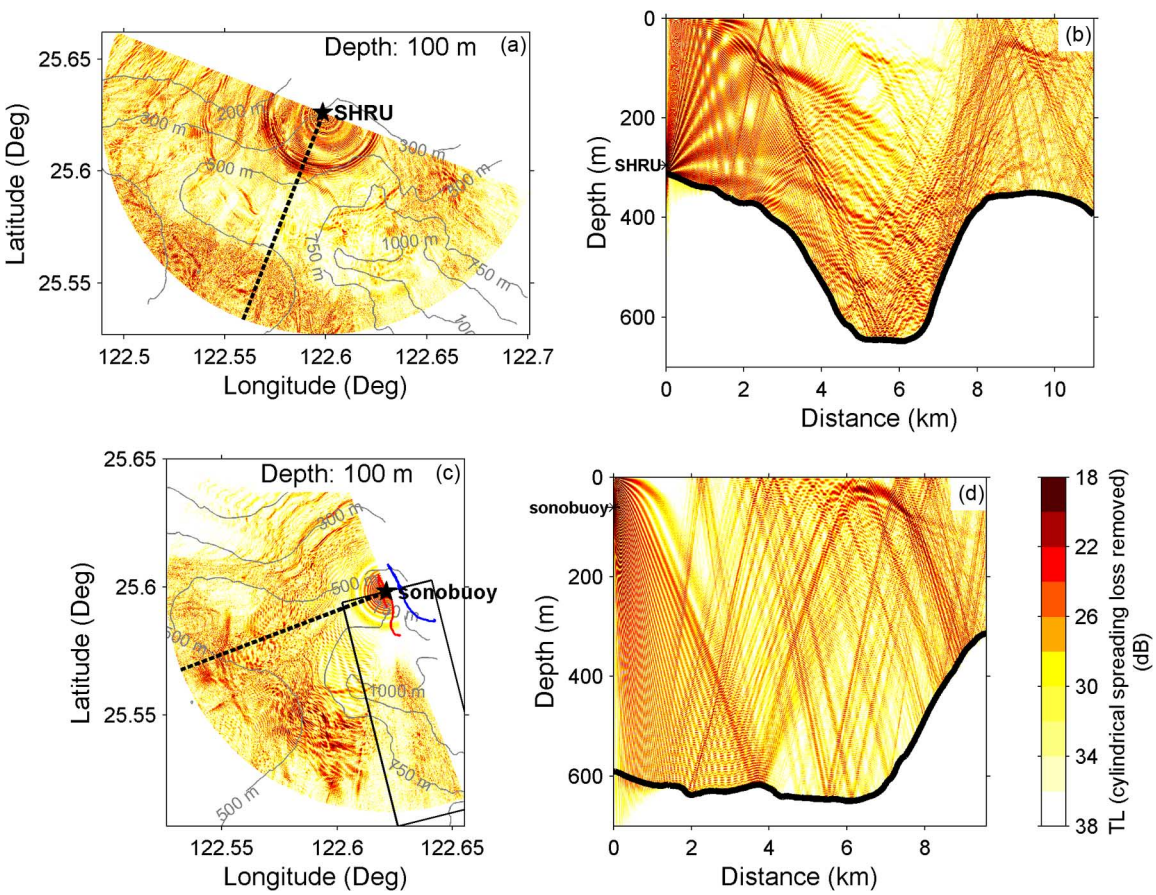

Fig. 12. Three-dimensional PE models of 800-Hz CW sound TL for two different receiver locations. Panels (a) and (b) show the TL to the SHRU array, and panels (c) and (d) show the TL to the sonobuoy hydrophone. The shaded images in panels (a) and (c) are the TL on a horizontal plane at 100-m depth, and panels (b) and (c) are the TL on a vertical plane along the central axis of the model domain. The box in panel (c) marks the model domain shown Fig. 3.

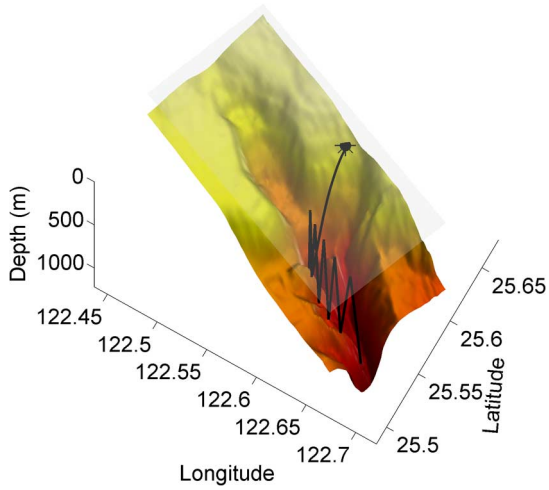

Fig. 13. Three-dimensional ray tracing of sound emitted from the SHRU location in the North Mien-Hua Canyon. The initial azimuth angle of the ray path is 30° with respect to the dashed line in Fig. 12(a), and its initial elevation angle is 7°.

angle and bottom properties, and this is discussed further in Section IV.

The 3-D PE numerical program was also utilized to simulate the TL of the OMAS 800-Hz CW signals received on one of the sonobuoys deployed to track the OMAS vehicle. The sonobuoys drifted freely, and their paths are plotted in Fig. 12(c). The sonobouys were in the area where the water depth is greater than 500 m, and the hydrophone depth was at 61 m. Fig. 12(c) shows the modeled TL for a given sonobuoy location, and the TL pattern is much different from the model for the SHRU array [Fig. 12(a)]. The reason is that both the source and the receiver were in the deep water area, and the shadow zone was narrower and closer to the receiver, as seen in a comparison between Fig. 12(b) and (d). Also note the box in Fig. 12(c) marking a focusing pattern. This has been, in fact, shown in the numerical example in Section III-A, and is caused by 3-D focusing of sound due to the concave canyon seafloor.

Last, $N\times$ 2-D PE models were implemented for modeling the SHRU data to compare with 3-D models. The goal was to study the strength of horizontal refraction for sound propagating across the canyon by differencing the 3-D and $N\times$ 2-D solutions. It was found that the horizontal refraction does not significantly affect the sound intensity for sound propagation across the canyon. A numerical program was then employed to solve the 3-D eikonal equation [14] for the ray paths emitted from the SHRU location in Run 2 to cross the canyon. Due to the out-of-plane reflection from the seafloor, some of the rays did, in fact, bounce into the canyon valley; see Fig. 13. This indicates that the horizontal refraction can occur for sound propagating across the canyon, but the refracted sound is greatly attenuated due to multiple bottom bounces. This is the reason why the sound intensity predicted from the 3-D PE model for sound propagation across the canyon did not show a significant effect due to horizontal refraction.

IV. Discussion

Environmental uncertainties in the 3-D sound propagation models for the OMAS canyon runs are addressed in this section. Although this uncertainty analysis is preliminary, it still produces some important results that can guide future research directions.

The first environmental uncertainty to be discussed is the bathymetry, which is the most important factor causing sound field complexity over a submarine canyon. Because bathymetric errors can transfer into TL errors through incorrect bottom interaction in a sound propagation model, it is important to have an accurate bathymetric map to ensure model accuracy. To examine the pre-QPE bathymetric database used in this paper, the water depth data obtained from shipboard echo sounders during the 2009 QPE cruises were compared. As shown in Fig. 14, bathymetric errors are, in fact, quite large. The area in the figure is around the OMAS canyon tracks (dashed lines on the maps) at the head of the west branch of the North Mien-Hua Canyon. The pre-QPE database does contain the beginning of the bathymetric bifurcation at around 25.55° N and 122.625° E, but it misses the details of the bifurcation. A line comparison along a ship track (the dark thick line on both maps) is provided in Fig. 14(c), and the disagreement is larger on the north into the bifurcation. The ship tracks are indicated by the thin lines on the QPE echo sounder map in Fig. 14(b). Because of the irregular and spatially sparse tracks, assimilating the echo sounder data into the bathymetric database is a challenge and is unlikely to significantly improve the modeled match to reality in an extended region; improvements are, therefore, deferred to a more thorough study in the future.

A specific comparison (Fig. 15) is made to show the difference in the modeled TL predictions resulted from using the two different bathymetric data sets. The propagation path considered, shown as the gray line in Fig. 14(a) and (b), runs across the canyon from the Run 2 SHRU location. The numerical computation considers sound propagation only in the vertical plane along the propagation path. The bathymetric data along this path differ substantially, as shown in Fig. 15, where it can be seen that the pre-QPE database misses the sharp cuts of the topography. These two bathymetric data sets indeed produce different TL predictions. The most notable discrepancy is the interference pattern near the start of the track, but both models produce comparable shadow zones ranging from 4 to 7 km and extending to 200-m depth. This explains why the data and model comparison in Fig. 11 shows reasonable agreement, even though the bathymetric database used in the model is not entirely correct. Also note the bottom reflection in the steep canyon [Fig. 15(b)]; although the up-slope propagation terminates the shadow zone, the TL is large because the steep slope causes greater bottom loss. This provides a reason why the OMAS Run 2 sound pressure levels were weak when the source left the shadow zone and moved to the southern side of the canyon from 13:00:00 to 14:00:00 (see Fig. 6).

The next environmental uncertainty to be considered is the bottom geoacoustic properties. Based on the understanding of strong currents in the canyon area, fine suspended sediments are not supposed to settle easily. So, a sandy bottom model is employed in the numerical simulations presented in the preceding section, with sound speed c_p 1700 m/s, density ρ_b 1.5 g/cm^3, and attenuation coefficient α_b 0.5 dB/λ. To present changes of the modeled TL due to different bottom properties, the same numerical computation for the OMAS Run 2 transmission (Fig. 11) is repeated with two other bottom sound speeds: 1600 and 1800 m/s. The resulting pdfs of modeled TL and comparisons to the measured mean TL data are shown in Fig. 16. The bottom model with $c_p = 1800$ m/s does improve the TL comparison. This

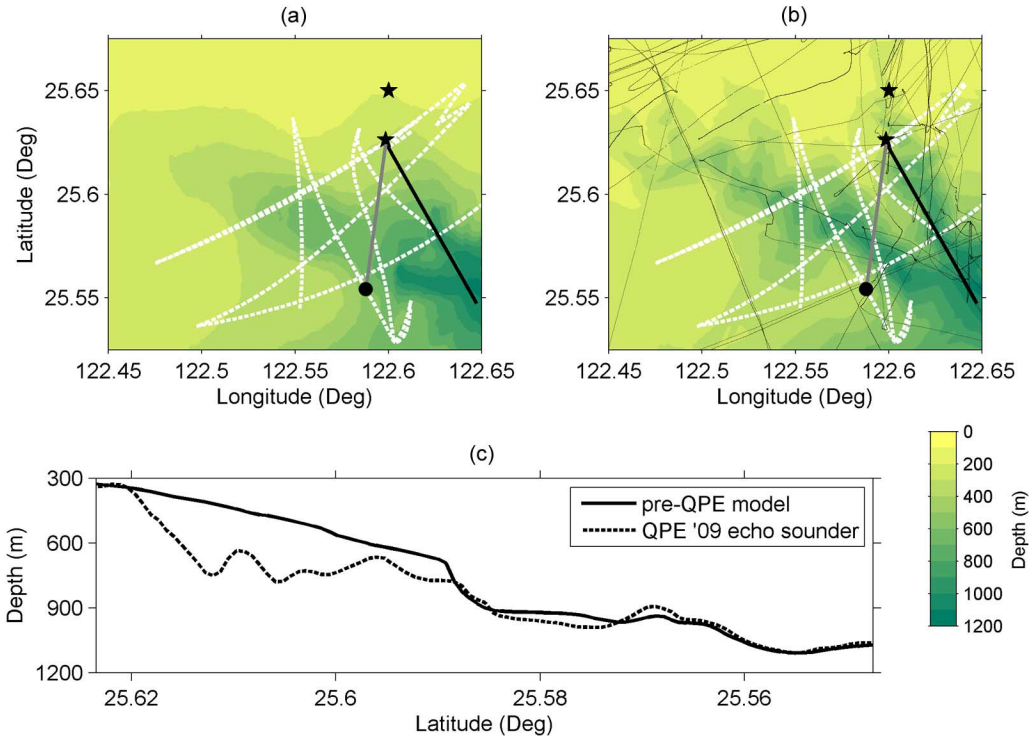

Fig. 14. Comparison of (a) the pre-QPE bathymetric database and (b) the QPE echo sounder data. (c) The bathymetry comparison along the dark thick line.

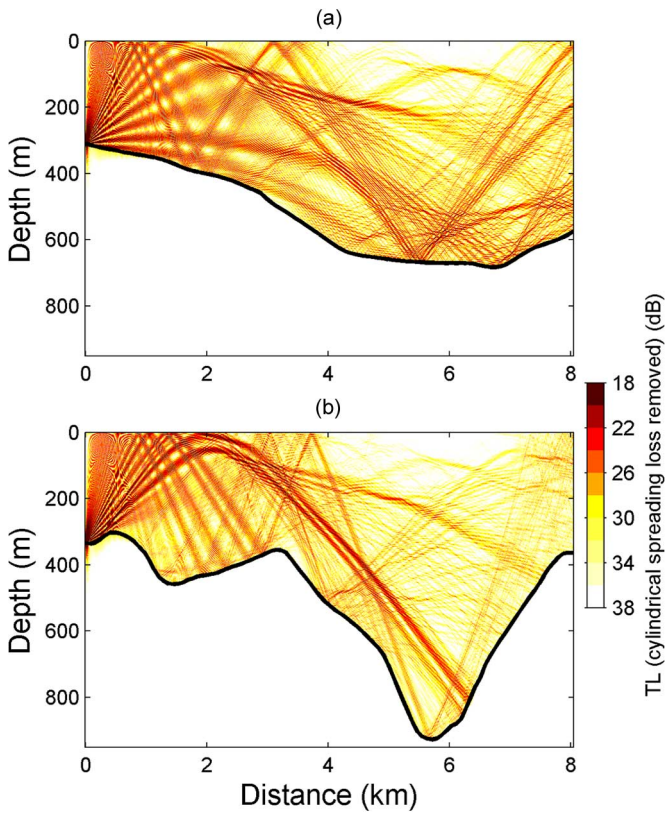

Fig. 15. Comparison of TL predictions resulted from two different bathymetric data: (a) the pre-QPE database and (b) the QPE echo sounder data.

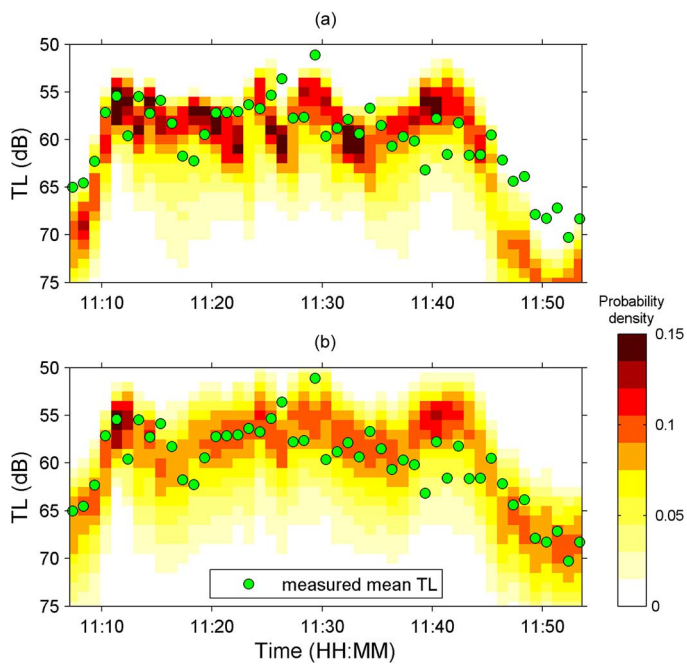

Fig. 16. Comparison of TL predictions using two bottom models with different bottom sound speeds c_p from the one used in Fig. 11(c): (a) $c_p = 1600$ m/s and (b) $c_p = 1800$ m/s. Note the bottom sound speed used in Fig. 11(c) is 1700 m/s.

suggests that the real bottom is probably harder than what we expect, or that the bottom is more variable (i.e., consists of a number of different regimes) than was assumed. To make a stronger statement, we need to consider the bathymetric uncertainty that can also affect the predictability of bottom reflections, as shown in Fig. 15. Such a joint uncertainty study is beyond the scope of this paper, and it is proposed for future work.

The last environmental uncertainty, also the most difficult one to address, is water–column variability. The oceanographic dynamics in the QPE experimental area are very complex with considerable temporal and spatial variability [1]. As shown in Fig. 2, vertical profiles of sound speed were sampled within the canyon along the central axis, but not across the canyon.

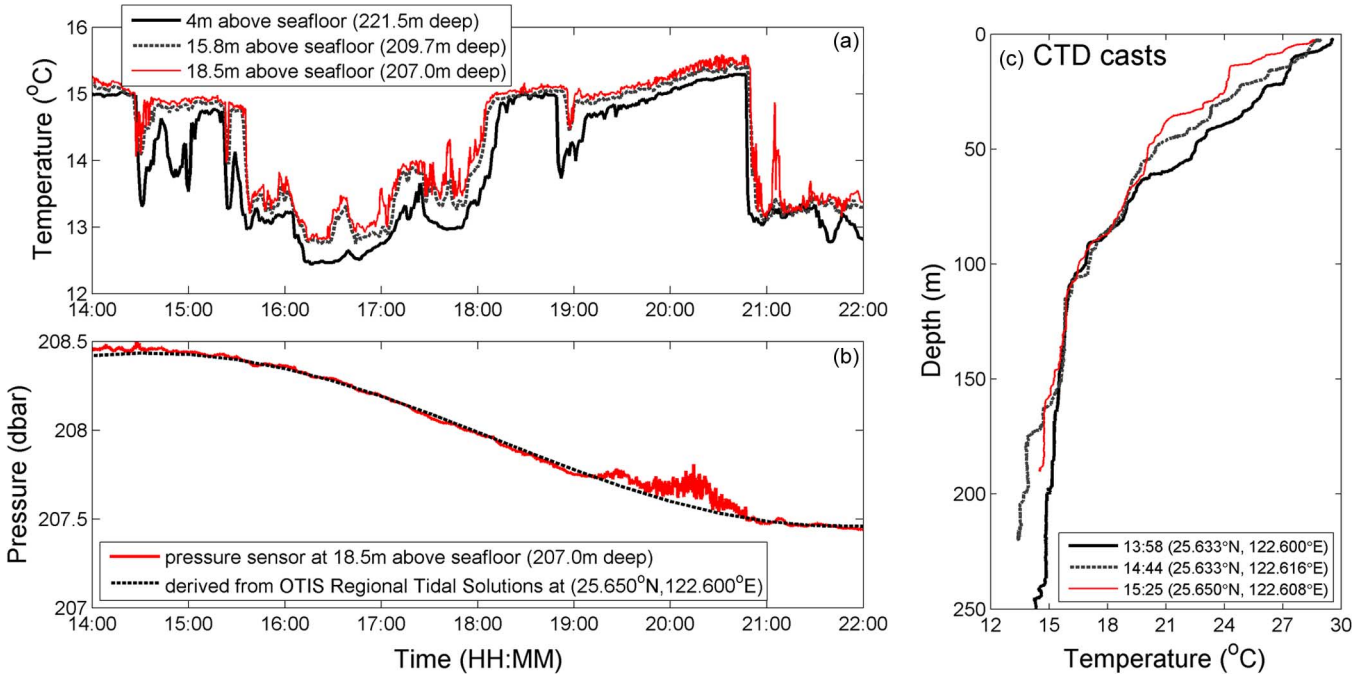

Fig. 17. (a) and (b) Temperature and pressure data obtained from the sensors on the SHRU mooring during the period of OMAS Run 1 transmission. (c) Temperature profiles obtained from three CTD casts around the SHRU location during the same period. The times and the locations that the casts were made are shown in the labels.

Specifically, the major sources of water–column fluctuations at the canyon site include barotropic and baroclinic tides/waves [15], [16], upwelling currents in the canyon and intrusions of the Kuroshio current [1], [17], [18]. In addition, the passage of Typhoon Morakot several weeks prior (August 6–8, 2009) also resulted in pulses of typhoon-induced runoff that affected the mixed layer depth and vertical gradients of sound speed within the canyon [19]. Thus, the spatially invariant vertical profile used in the numerical simulations does not express the real sound-speed variability within the canyon. This can bias TL model predictions especially, as discussed below, in the presence of nonlinear internal waves that can scatter sound [20], cause horizontal refraction [21], and produce 3-D sound propagation effects [22]. Nevertheless, the acoustic models presented in this paper capture topographic effects with a general downward-refracting propagation condition in the water column, which is the first step in addressing the acoustic propagation within the canyon.

One interesting section of the SPL data seen in the OMAS Run 1 transmission (Fig. 5) was recorded when the OMAS source traveled through the zigzag track in the east of the SHRU location from 18:20:00 to 19:30:00 [see Fig. 2(a)]. The signal levels of OMAS CW tones during this period dropped drastically ($>$15 dB) and almost reached the noise floor at $\sim$60 dB re 1 μPa. The time series of the SPL data appeared just as the OMAS entered a shadow zone like the other cases explained in Section III, but numerical simulations with the average sound-speed profile did not support this hypothesis. In fact, it was found to be more likely due to nonlinear internal waves, and a brief discussion is provided below.

Fig. 17 shows the water temperature and pressure data during the OMAS Run 1 transmission, measured by the sensors attached to the SHRU mooring. The sensors were placed close to the bottom (the depths are labeled in the plot), and the temperature varied significantly. The pressure data were less variable, indicating little mooring motion, and they, in fact, followed closely with the regional barotropic tidal levels obtained from the Oregon State University Tidal Inversion Software (OTIS, available at http://volkov.oce.orst.edu/tides/YS.html). Although the mooring did not extend to the upper part of the water column, there were three CTD casts made near the mooring within 2 km [see Fig. 2(a)], and we can use those CTD profiles, shown in Fig. 17(c), to infer the thermocline displacement in the upper water. The CTD casts were made in one and a half hours between 14:00:00 and 15:30:00, during which the water temperature near the bottom varied between 13 °C and 15 °C. Meanwhile, the displacement of the thermocline was over 30 m, which was most likely due to nonlinear internal waves. Now, shift attention back to the temperature time series from 18:30:00 to 19:30:00 when the acoustic signal levels dropped drastically. Apparent changes with a wavelike pattern can be observed on the water temperature data in Fig. 17(a), suggesting that a train of nonlinear internal waves passed through the mooring site. This provides a reason why the acoustic signal levels dropped so much, as the sound attenuation due to scattering by nonlinear internal waves can be considerable [20]. Although we did not have full water–column profiles to simulate sound propagation through the internal waves, the arguments presented here should be strong enough to point out the importance of water–column uncertainty on acoustic TL predictions.

V. Conclusion

Experimental and numerical studies have been conducted for sound propagation over the North Mien-Hua Canyon northeast of Taiwan. A precruise numerical study showed a strong 3-D focusing effect caused by the concave canyon seafloor. Mobile acoustic sources were deployed to validate the model. However, the sources were pushed off of their planned tracks by the current, so we were not able to confirm the predicted focusing effect. Nonetheless, the field data still showed a shadowing ef-

fect, which is also an important factor in considering underwater sound propagation over a submarine canyon.

A 3-D PE model has been utilized to provide physical insights into the TL data. Acoustic shadow zones are identified in the numerical model, and the resultant shadowing effect agrees with the measured data quite well. Model uncertainties due to incomplete measurements of the sound-speed field, the seafloor topography and the sub-bottom structure are also noted, and it is left for future work to thoroughly evaluate the effect of each environmental uncertainty on the TL predictability. Bathymetric uncertainty could be the most important factor when considering sound propagation in a submarine canyon, and it will affect the TL predictions in conjunction with other environmental uncertainties. Incorporating ocean dynamic models to reduce water–column uncertainty is suggested and currently being pursued by the authors and their collaborators. Last, our 3-D sound propagation model suggests that strong focusing of sound will occur along the canyon axis, but it still remains to be validated in a real environment.

Acknowledgment

The authors would like to thank all the Principal Investigators on both Taiwan and U.S. sides of the Quantifying, Predicting and Exploiting (QPE) Uncertainty Initiative Experiment for their incredible efforts on this international collaboration. They would also like to thank the U.S. Office of Naval Research (ONR) program managers Dr. C.-S. Chiu, Dr. D. B. Reeder, Dr. E. S. Livingston, Dr. T. Paluszkiewicz, and Dr. D. Marble for their support. The cruise members of the *R/V OR1* during the North Mien-Hua Canyon test, especially D. Morton of OASIS Inc. (Lexington, MA, USA), are sincerely acknowledged.

References

[1] G. Gawarkiewicz, S. Jan, P. F. J. Lermusiaux, J. L. McClean, L. Centurioni, K. Taylor, B. Cornuelle, T. F. Duda, J. Wang, Y. J. Yang, T. Sanford, R.-C. Lien, C. Lee, M.-A. Lee, W. Leslie, P. J. Haley, Jr., P. P. Niiler, G. Gopalakrishnan, P. Velez-Belchi, D.-K. Lee, and Y. Y. Kim, "Circulation and intrusions northeast of Taiwan: Chasing and predicting uncertainty in the cold dome," *Oceanography*, vol. 24, pp. 110–121, 2011.

[2] L. Y. S. Chiu, Y.-T. Lin, C.-F. Chen, T. F. Duda, and B. Calder, "Focused sound from three-dimensional sound propagation effects over a submarine canyon," *J. Acoust. Soc. Amer.*, vol. 129, pp. EL260–EL266, 2011.

[3] J. S. Lim, *Two-Dimensional Signal and Image Processing*. Englewood Cliffs, NJ, USA: Prentice-Hall, 1990, pp. 469–476.

[4] A. E. Newhall, J. F. Lynch, G. Gawarkiewicz, T. F. Duda, N. M. McPhee, F. B. Bahr, C. D. Marquette, Y.-T. Lin, S. Jan, J. Wang, C.-F. Chen, L. Y.-S. Chiu, Y.-J. Yang, R.-C. Wei, C. Emerson, D. Morton, T. Abbot, P. Abbot, B. Calder, L. A. Mayer, and P. F. J. Lermusiaux, "Acoustics and oceanographic observations collected during the QPE experiment by research vessels OR1, OR2, and OR3 in the East China Sea in the summer of 2009," Woods Hole Oceanogr. Inst., Woods Hole, MA, USA, Tech. Rep., WHOI-2010-06, 2010.

[5] F. D. Tappert, "The parabolic approximation method," in *Wave Propagation and Underwater Acoustics*, J. B. Keller and J. S. Papadakis, Eds. Berlin, German: Springer-Verlag, 1977, pp. 224–287.

[6] M. D. Feit and J. A. Fleck, Jr., "Light propagation in graded-index fibers," *Appl. Opt.*, vol. 17, pp. 3990–3998, 1978.

[7] T. F. Duda, "Initial results from a Cartesian three-dimensional parabolic equation acoustical propagation code," Woods Hole Oceanogr. Inst., Woods Hole, MA, USA, Tech. Rep., WHOI-2006-041, 2006.

[8] Y.-T. Lin, T. F. Duda, and A. E. Newhall, "Three-dimensional sound propagation models using the parabolic-equation approximation and the split-step Fourier method," *J. Comput. Acoust.*, vol. 21, 2013, 1250018.

[9] P. Abbot, C. Gedney, D. Morton, and C. Emerson, "Mobile acoustic source for underwater acoustic measurements," in *Proc. IEEE/MTS OCEANS Conf.*, Boston, MA, USA, 2007, DOI: 10.1109/OCEANS.2006.307075.

[10] R. J. Urick, *Principles of Underwater Sound*, 3rd ed. New York, NY, USA: McGraw-Hill, 1983, ch. 7.

[11] H.-M. Zhang, J. J. Bates, and R. W. Reynolds, "Assessment of composite global sampling: Sea surface wind speed," *Geophys. Res. Lett.*, vol. 33, 2006, L17714.

[12] H.-M. Zhang, R. W. Reynolds, and J. J. Bates, "Blended and gridded high resolution global sea surface wind speed and climatology from multiple satellites: 1987–present," in *Proc. Amer. Meteorol. Soc. Annu. Meeting*, Atlanta, GA, USA, 2006, Paper #P2.23.

[13] I. Dyer, "Statistics of sound propagation in the ocean," *J. Acoust. Soc. Amer.*, vol. 48, pp. 337–345, 1970.

[14] F. B. Jensen, W. A. Kuperman, M. B. Porter, and H. Schmidt, *Computational Ocean Acoustics*. New York, NY, USA: AIP, 1994, ch. 3.

[15] T. F. Duda, A. E. Newhall, G. Gawarkiewicz, M. J. Caruso, H. C. Graber, Y. J. Yang, and S. Jan, "Significant internal waves and internal tides measured northeast of Taiwan," *J. Mar. Res.*, vol. 71, pp. 47–81, 2013.

[16] R.-C. Lien, T. Sanford, S. Jan, M.-H. Chang, and B. Ma, "Internal tides of the East China Sea continental slope," *J. Mar. Res.*, vol. 71, pp. 151–185, 2013.

[17] S. Jan, C.-C. Chen, Y.-L. Tsai, Y.-J. Yang, J. Wang, C.-S. Chern, G. Gawarkiewicz, R.-C. Lien, and J.-L. Kuo, "Mean structure and variability of the Cold Dome northeast of Taiwan," *Oceanography*, vol. 24, pp. 100–109, 2011.

[18] P. Velez-Belchi, L. Centurioni, D.-K. Lee, S. Jan, and P. P. Niiler, "Eddy induced Kuroshio Intrusions onto the continental shelf of the East China Sea," *J. Mar. Res.*, vol. 71, pp. 83–107, 2013.

[19] S. Jan, J. Wang, Y.-J. Yang, C.-C. Hung, C.-S. Chern, G. Gawarkiewicz, R.-C. Lien, and L. Centurioni, "Observations of a freshwater pulse induced by Typhoon Morakot off the northern coast of Taiwan in August, 2009," *J. Mar. Res.*, vol. 71, pp. 19–46, 2013.

[20] J. Zhou, X. Zhang, and P. H. Rogers, "Resonant interaction of sound wave with internal solitons in the coastal zone," *J. Acoust. Soc. Amer.*, vol. 90, pp. 2042–2054, 1991.

[21] M. Badiey, B. G. Katsnelson, Y.-T. Lin, and J. F. Lynch, "Acoustic multipath arrivals in the horizontal plane due to approaching nonlinear internal waves," *J. Acoust. Soc. Amer.*, vol. 129, pp. EL141–EL147, 2011.

[22] M. Badiey, B. G. Katsnelson, J. F. Lynch, S. Pereselkov, and W. L. Siegmann, "Measurement and modeling of three-dimensional sound intensity variations due to shallow-water internal waves," *J. Acoust. Soc. Amer.*, vol. 117, pp. 613–625, 2005.

Ying-Tsong Lin (M'10) received the B.S. degree in hydraulic and ocean engineering from the National Cheng Kung University, Tainan City, Taiwan, in 1996 and the M.S. degree in naval architecture and ocean engineering and the Ph.D. degree in engineering science and ocean engineering from the National Taiwan University (NTU), Taipei City, Taiwan, in 1998 and 2004, respectively.

From 2002 to 2003, he was a Guest Investigator in the Applied Ocean Physics & Engineering (AOP&E) Department, Woods Hole Oceanographic Institution (WHOI), Woods Hole, MA, USA. After receiving his Ph.D. degree, he began a half-year postdoctoral appointment at the Underwater Acoustics Laboratory, NTU, after which he worked at WHOI as a Postdoctoral Researcher. He currently holds the position of an Associate Scientist in the AOP&E Department of WHOI. His research interests include shallow-water acoustic propagation, acoustical oceanography, geoacoustic inversion, and underwater sound source localization.

Dr. Lin is a member of the IEEE Oceanic Engineering Society, the Acoustical Society of America, and the American Geophysical Union.

Timothy F. Duda (M'05–SM'09) received the B.A. degree in physics from Pomona College, Claremont, CA, USA, in 1979 and the Ph.D. degree in oceanography from the Scripps Institution of Oceanography, University of California San Diego, La Jolla, CA, USA, in 1986.

He worked at the University of California Santa Cruz, Santa Cruz, CA, USA, from 1986 to 1991. He has been a Scientist at the Woods Hole Oceanographic Institution, Woods Hole, MA, USA, since 1991. His three primary fields of study are ocean acoustic propagation, ocean internal gravity waves, and ocean mixing processes. His research has included physical process studies, development of new measurement tools, and computational acoustic modeling.

Dr. Duda is a member of the IEEE Oceanic Engineering Society. He is also a member of the American Meteorological Society, the American Geophysical Union, and the Acoustical Society of America.

Chris Emerson received the M.S. degree in ocean engineering from the Massachusetts Institute of Technology, Cambridge, MA, USA, in 2000.

He is a Senior Engineer at Ocean Acoustical Services and Instrumentation Systems (OASIS), Inc., Lexington, MA, USA. His areas of interest include shallow-water acoustics, hydrodynamics, and autonomous underwater vehicle (AUV) development.

Glen Gawarkiewicz received the B.S. degree in ocean engineering from the Massachusetts Institute of Technology, Cambridge, MA, USA, in 1981 and the Ph.D. degree in physical oceanography from the University of Delaware, Newark, DE, USA, in 1989.

He is a Senior Scientist at the Woods Hole Oceanographic Institution (WHOI), Woods Hole, MA, USA. His interests include continental shelf and slope processes, frontal dynamics, application of autonomous underwater vehicle (AUV) technology to oceanographic research, and development of oceanographic observatories.

Arthur E. Newhall (M'07) received the B.S. degree in mathematics from the University of Maine at Orono, Orono, ME, USA, in 1985.

He is an Information System Specialist in the Applied Ocean Physics and Engineering Department, Woods Hole Oceanographic Institution (WHOI), Woods Hole, MA, MA. His current interests include ocean acoustic propagation modeling, acoustical oceanography, software engineering, and music.

Mr. Newhall is a member of the Acoustical Society of America.

Brian Calder (M'04) received the M.Eng (with Merit) and Ph.D. degrees in electrical and electronic engineering from Heriot-Watt University, Edinburgh, Scotland, in 1994 and 1997, respectively.

Since January 2000, he has been with the Center for Coastal and Ocean Mapping (CCOM) and NOAA-UNH Joint Hydrographic Center, University of New Hampshire, Durham, NH, USA, where he specializes in algorithms and methods for hydrographic data processing with particular emphasis on uncertainty management. He is an Associate Research Professor in Ocean Engineering and Associate Director of CCOM.

Dr. Calder was previously an Associate Editor of the IEEE JOURNAL OF OCEANIC ENGINEERING.

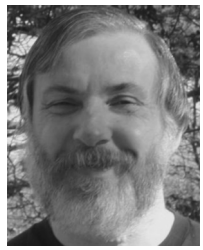

James F. Lynch (M'96–SM'02–F'05) received the B.S. degree in physics from Stevens Institute of Technology, Hoboken, NJ, USA, in 1972 and the Ph.D. degree in physics from the University of Texas at Austin, Austin, TX, USA, in 1978.

He then worked for three years at the Applied Research Laboratories, University of Texas at Austin (ARL/UT) from 1978 to 1981, after which he joined the scientific staff at the Woods Hole Oceanographic Institution (WHOI), Woods Hole, MA, USA. He has worked at WHOI since then, and currently holds the position of Senior Scientist. His research specialty areas are ocean acoustics and acoustical oceanography. He also greatly enjoys occasional forays into physical oceanography, marine geology, and marine biology.

Dr. Lynch is a Fellow of the Acoustical Society of America, a former Editor-in-Chief of the IEEE JOURNAL OF OCEANIC ENGINEERING, and current Editor-in-Chief of the *Journal of the Acoustical Society of America Express Letters*.

Philip Abbot (M'99) received the M.S. degree in ocean engineering from the Massachusetts Institute of Technology, Cambridge, MA, USA, in 1979.

He is the President of Ocean Acoustical Services and Instrumentation Systems (OASIS), Inc., Lexington, MA, USA, where he handles overall marketing and technical performance. His primary interests are in the areas of shallow-water ocean acoustics and sonar array design, hydroacoustics and weapon silencing, and cavitation detection and monitoring.

Yiing-Jang Yang was born in Taiwan in 1967. He received the B.S. degree in oceanography from the National Taiwan Ocean University, Keelung, Taiwan, in 1990 and the Ph.D. degree in physical oceanography from the National Taiwan University, Taipei, Taiwan, in 1996.

Currently, he is an Associate Professor at the Institute of Oceanography, National Taiwan University. His research interests include internal tides and waves, and current variation around Taiwan.

Dr. Yang is a Member of the American Geophysical Union.

Sen Jan received the B.S. degree in mechanical engineering from Chung Yung University, Zhongli City, Taiwan, in 1986 and the M.S. and Ph.D. degrees in physical oceanography from the National Taiwan University, Taipei, Taiwan, in 1988 and 1995, respectively.

He is a Professor at the Institute of Oceanography, National Taiwan University. His research interests are dynamics of internal tides in the Luzon Strait and northern South China Sea, and dynamics for the fluctuation of the North Pacific western boundary current (the Kuroshio) east of Taiwan. He adopts both *in situ* measurement and numerical modeling to study oceanic processes.

Dr. Jan is a Member of the American Geophysical Union.